# Conservative Finite Volume Schemes for Meteorological Applications

Rupert Klein

Mathematik & Informatik, Freie Universität Berlin
Data & Computation, Potsdam Institute for Climate Impact Research

| | |
|---|---|
| Emmanuel Audusse | (Paris 13) |
| Ann Almgren | (Lawrence Berkeley Lab.) |
| Nicola Botta | (PIK) |
| Michael Minion | (UNC-Chapel Hill) |
| Claus-Dieter Munz | (Uni-Stuttgart) |
| Antony Owinoh | (FUB / PIK) |
| Stefan Vater | (FUB / PIK) |

***Thanks to ...***

## Motivation

Balancing gravity

Momentum conservation vs. Coriolis

A low-Mach / low-Froude conservative scheme

- low Mach number Godunov-Type scheme
- robust, exact projection
- low-Froude extension

$$
\begin{aligned}
\boldsymbol{u}_t + \boldsymbol{u}\cdot\nabla\boldsymbol{u} + w\boldsymbol{u}_z + \nabla\pi &= \boldsymbol{S_u}\\
w_t + \boldsymbol{u}\cdot\nabla w + w w_z + \pi_z &= -\theta' + S_w\\
\theta'_t + \boldsymbol{u}\cdot\nabla\theta' + w\theta'_z &= S'_\theta\\
\nabla\cdot(\rho_0\boldsymbol{u}) + (\rho_0 w)_z &= 0
\end{aligned}
$$

$$\theta = 1 + \varepsilon^4\theta'(\boldsymbol{x}, z, t) + o(\varepsilon^4)$$

***Anelastic Boussinesque Model***

**10 km / 20 min**

$$\left(\partial_\tau + \boldsymbol{u}^{(0)}\cdot\nabla\right) q = 0$$

$$q = \zeta^{(0)} + \Omega_0\beta\eta + \frac{\Omega_0}{\rho^{(0)}}\frac{\partial}{\partial z}\left(\frac{\rho^{(0)}}{d\Theta/dz}\theta^{(3)}\right)$$

$$\zeta^{(0)} = \nabla^2\pi^{(3)}, \qquad \theta^{(3)} = -\frac{\partial\pi^{(3)}}{\partial z}, \qquad \boldsymbol{u}^{(0)} = \frac{1}{\Omega}\boldsymbol{k}\times\nabla\pi^{(3)}$$

***Quasi-geostrophic theory***

**1000 km / 2 days**

$$
\begin{aligned}
\frac{\partial Q_T}{\partial t} + \nabla\cdot\boldsymbol{F}_T &= S_T\\
\frac{\partial Q_q}{\partial t} + \nabla\cdot\boldsymbol{F}_q &= S_q
\end{aligned}
$$

$$Q_\varphi = \int_{z_s}^{H_a}\rho\,\varphi\,dz\,, \qquad \boldsymbol{F}_\varphi = \int_{z_s}^{H_a}\rho\left(\boldsymbol{u}\,\varphi + (\widehat{\boldsymbol{u}'\,\varphi'}) + \boldsymbol{D}^\varphi\right)dz\,, \qquad \left(\varphi\in\{T, q\}\right)$$

$$T = T_s(t,\boldsymbol{x}) + \Gamma(t,\boldsymbol{x})\Big(\min(z, H_T) - z_s\Big)\,, \qquad q = q_s(t,\boldsymbol{x})\exp\left(-\frac{z - z_s}{H_q}\right)$$

$$\rho = \rho_*\exp\left(-\frac{z}{h_{\mathrm{sc}}}\right)\,, \qquad p = p_*\exp\left(-\frac{\gamma z}{h_{\mathrm{sc}}}\right) + p_0(t,\boldsymbol{x}) + g\rho_*\int_0^z\frac{T}{T_*}\,dz'$$

$$\boldsymbol{u} = \boldsymbol{u}_g + \boldsymbol{u}_a\,, \qquad f\rho_*\boldsymbol{k}\times\boldsymbol{u}_g = -\nabla_{\boldsymbol{x}}p \qquad \boldsymbol{u}_\alpha = \alpha\nabla p_0$$

V. Petoukhov et al., *CLIMBER-2 ...*, Climate Dynamics, 16, (2000)

***EMIC - equations (CLIMBER-2)***

**10000 km / 1 season**

# *Scales in the Atmosphere*

## Three-dimensional compressible flow equations

$$
\begin{aligned}
\rho_t \quad &+ \nabla\cdot(\rho\boldsymbol{v}) &&= 0\\
(\rho\boldsymbol{v})_t \quad &+ \nabla\cdot(\rho\boldsymbol{v}\circ\boldsymbol{v}) + \frac{1}{\mathbf{M}^2}\nabla p + \frac{1}{\mathbf{Ro}}\boldsymbol{\Omega}\times\rho\boldsymbol{v} &&= \boldsymbol{S}_{\rho\boldsymbol{v}} - \frac{1}{\mathbf{Fr}^2}\rho g\,\boldsymbol{k}\\
(\rho e)_t \quad &+ \nabla\cdot(\boldsymbol{v}\,[\rho e + p]) &&= S_{\rho e}\\
(\rho Y_j)_t &+ \nabla\cdot\big(\rho Y_j\boldsymbol{v}\big) &&= S_{\rho Y_j}
\end{aligned}
$$

$$
(\rho e) = \frac{p}{\gamma-1} + \frac{1}{2}\rho\boldsymbol{v}^2 + \rho\sum_{j=1}^{N} Q_j Y_j
$$

**Many asymptotic regimes — a single numerical scheme?**

*The "Truth"*

## Why conservation?

**The integral conservation law**

$$\int\limits_{\Omega} \Phi \, d\boldsymbol{x} \Bigg|_{t_1}^{t_2} = - \int\limits_{t_1}^{t_2} \oint\limits_{\partial\Omega} \boldsymbol{f}_{\Phi} \cdot \boldsymbol{n} \, d\sigma \, dt$$

**is uniformly valid for arbitrary control volumes**

$$\Downarrow$$

**Mathematically sound subgrid closures**

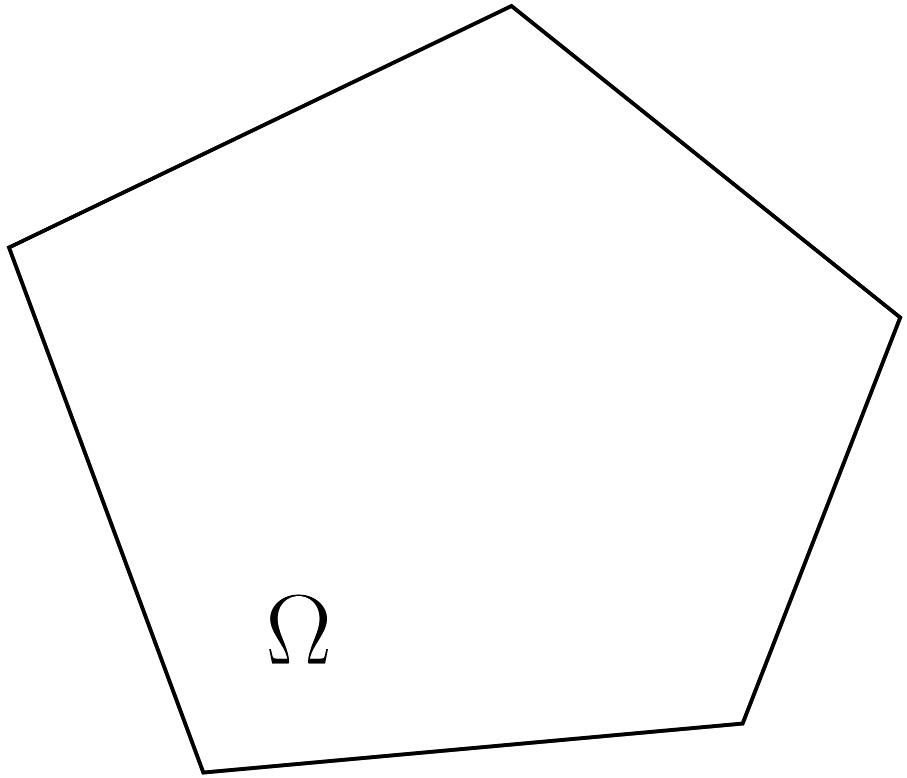

Motivation

**Balancing gravity**

Momentum conservation vs. Coriolis

A low-Mach / low-Froude conservative scheme

- low Mach number Godunov-Type scheme
- robust, exact projection
- low-Froude extension

## Spurious winds over steep orography

- **atmosphere at rest**
- **3000 m mountain**
- **3D compressible inviscid flow eqs.**
- **standard finite volume scheme**
- **128 $\times$ 32 grid cells**
- **velocities after about** $60\,\mathrm{min}$

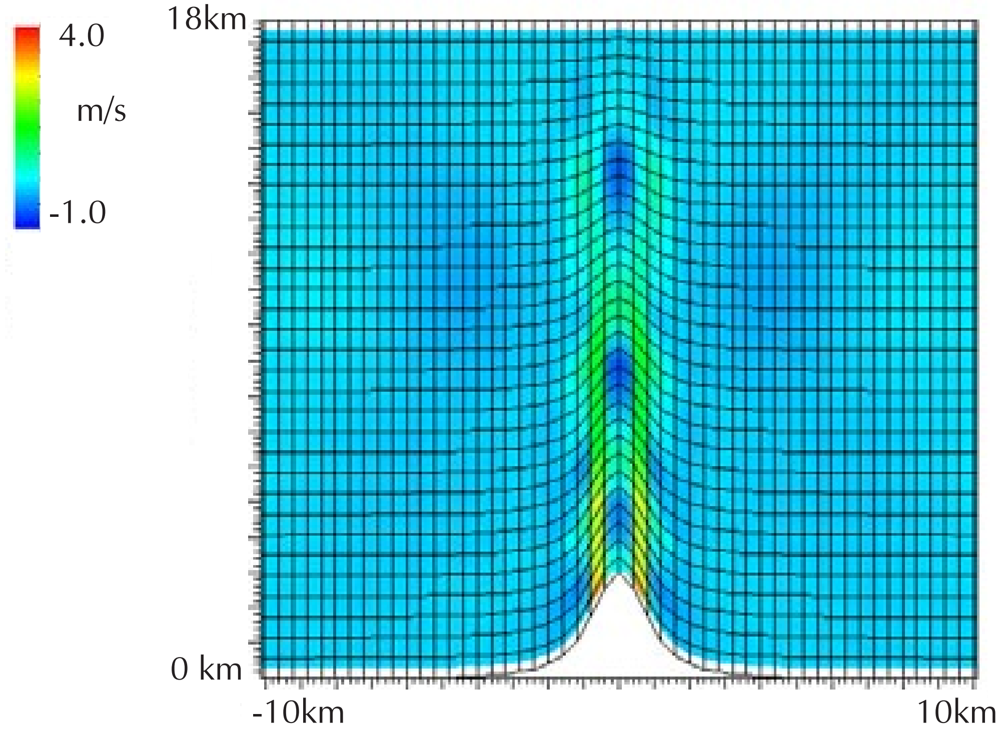


**Various finite difference / finite volume schemes produce comparable results.**

***Accumulation of unbalanced truncation errors***

- The background pressure / temperature structure of the atmosphere is (almost) everywhere dominated by hydrostatic balance.

- Mathematically, this follows from the distinguished limits

$$\mathbf{Fr}^2/\mathbf{M}^2 = O(1), \;\; \mathrm{Ro} \gg \mathbf{M}^2, \;\; (\mathbf{M} \to 0)$$

- Vertical momentum balance

$$(\rho w)_t + \nabla \cdot (\rho \boldsymbol{v} w) + \frac{1}{\mathrm{Ro}} \boldsymbol{k} \cdot (\boldsymbol{\Omega} \times \boldsymbol{v}) = -\left( \frac{1}{\mathbf{M}^2} \frac{\partial p}{\partial z} + \frac{1}{\mathbf{Fr}^2} \rho \right).$$

- Numerical truncation errors for 30 vertical layers, 2nd order scheme

$$(\delta w)_{\mathrm{num.}} = O\left( \frac{1}{\mathbf{M}^2} \Delta x^2 \right) \sim \frac{(1/30)^2}{(0.03)^2} \sim O(1)$$

## ***Origin of unbalanced truncation errors***

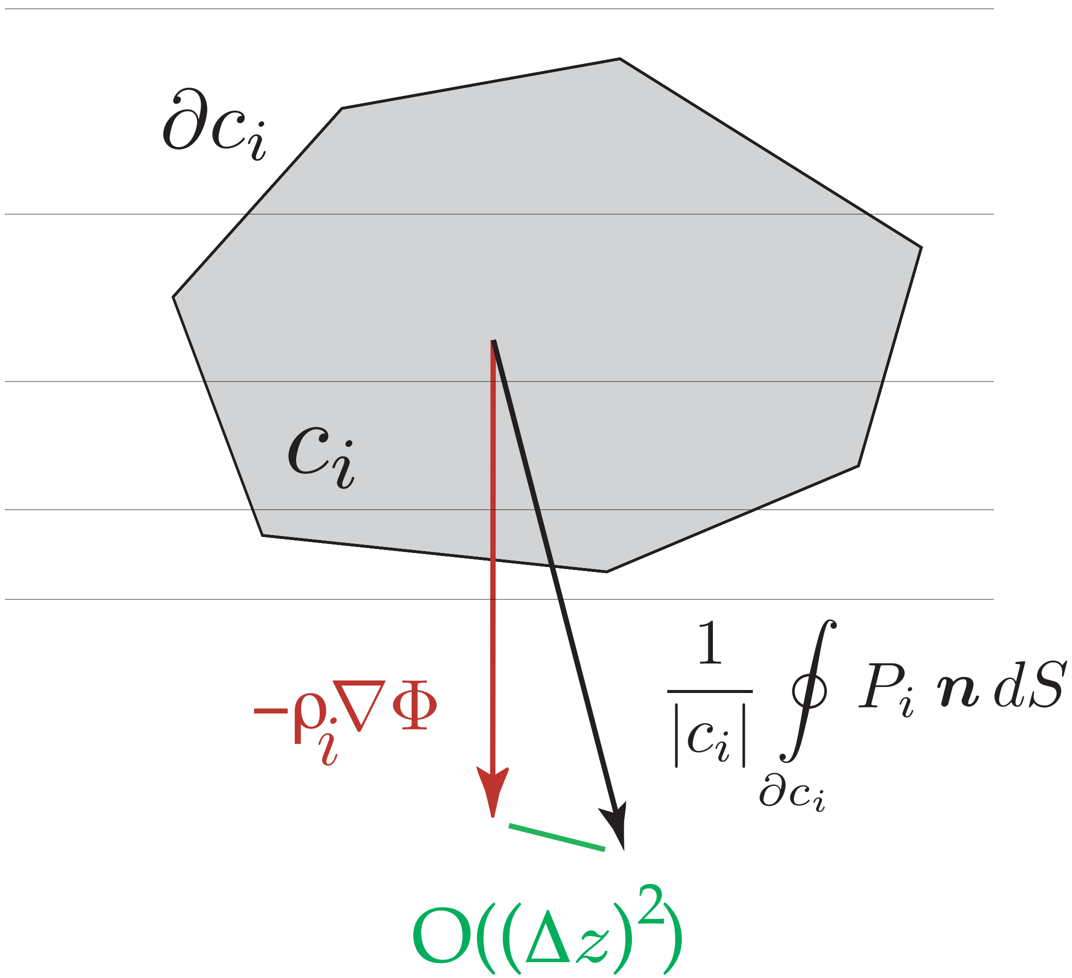


***Archimedes' principle***

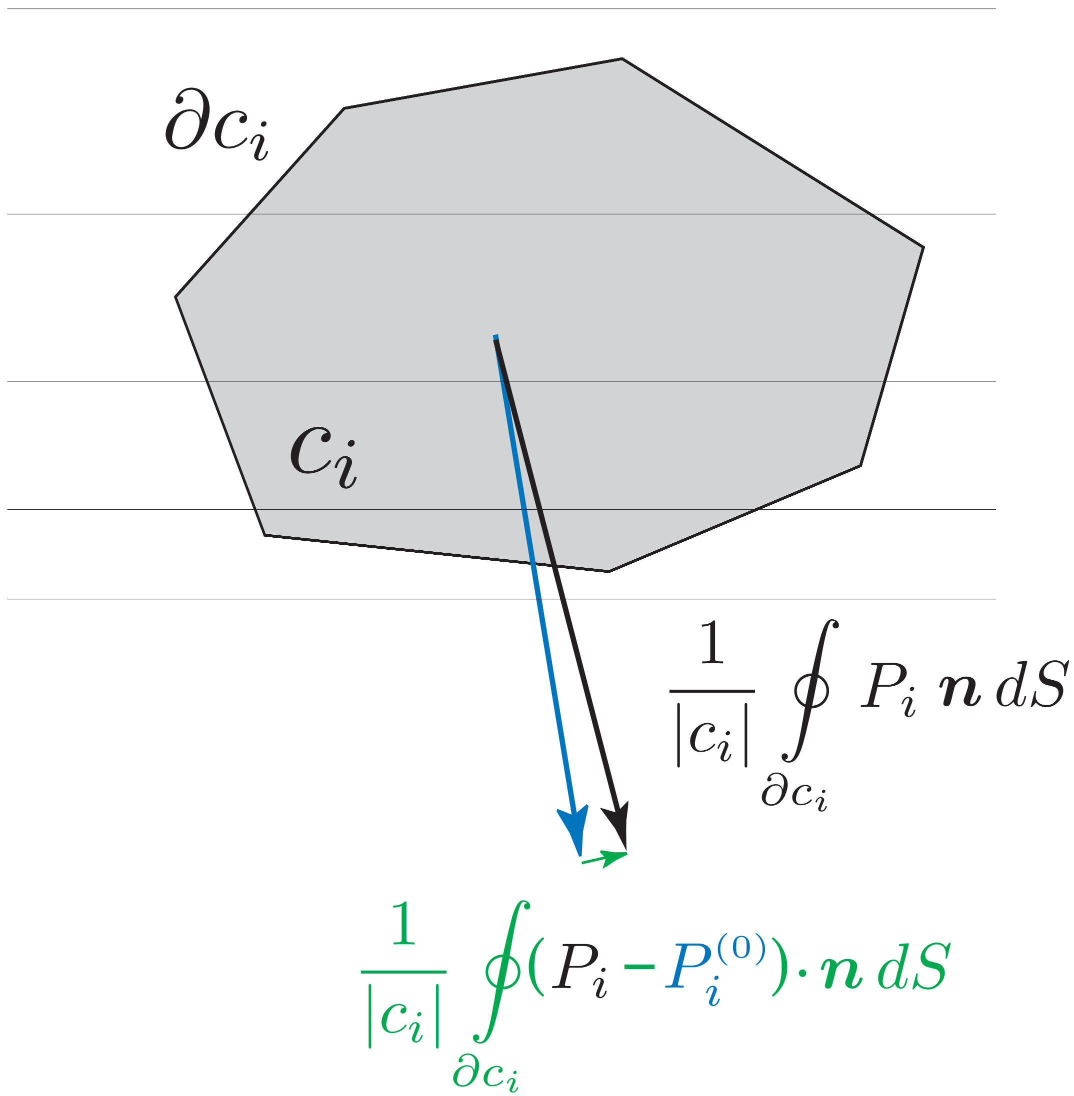


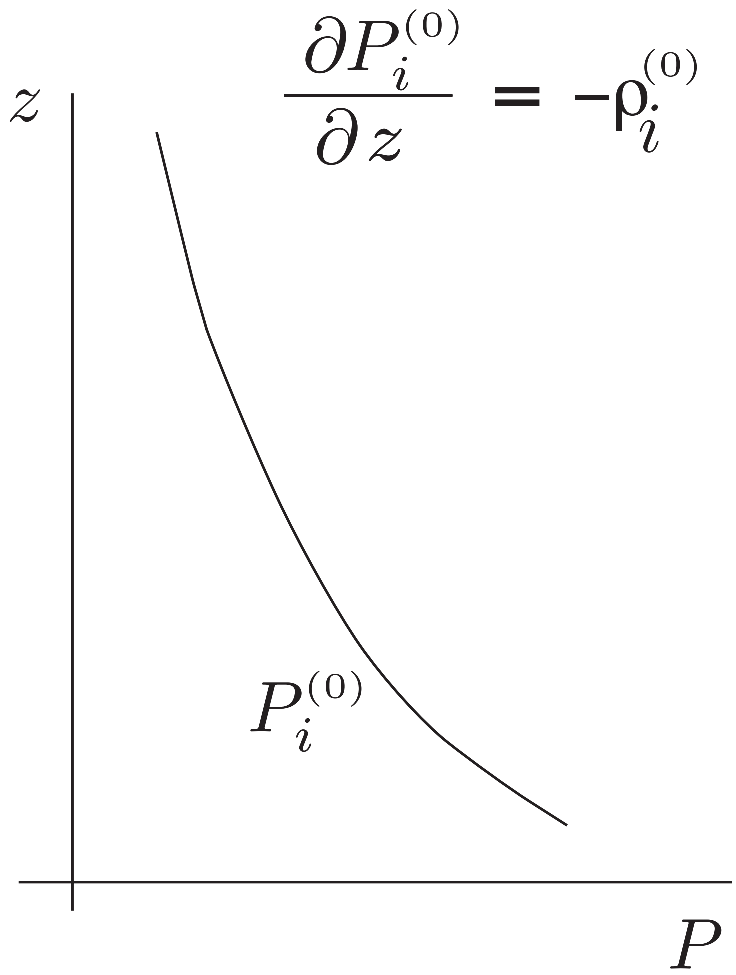


**Archimedes' principle**

# Piecewise linear potential temperature

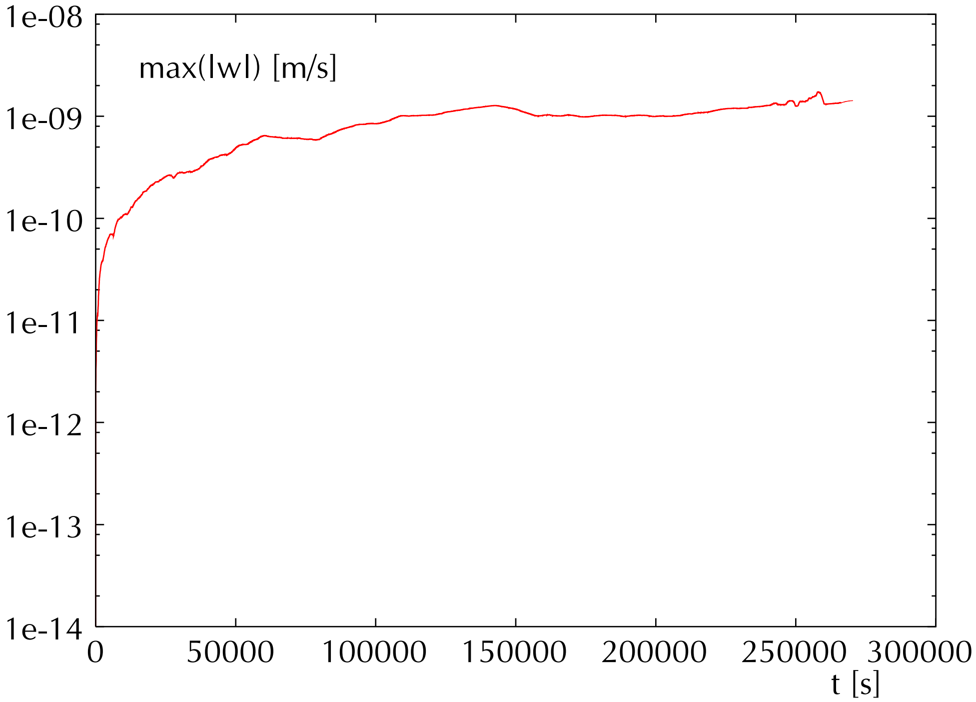


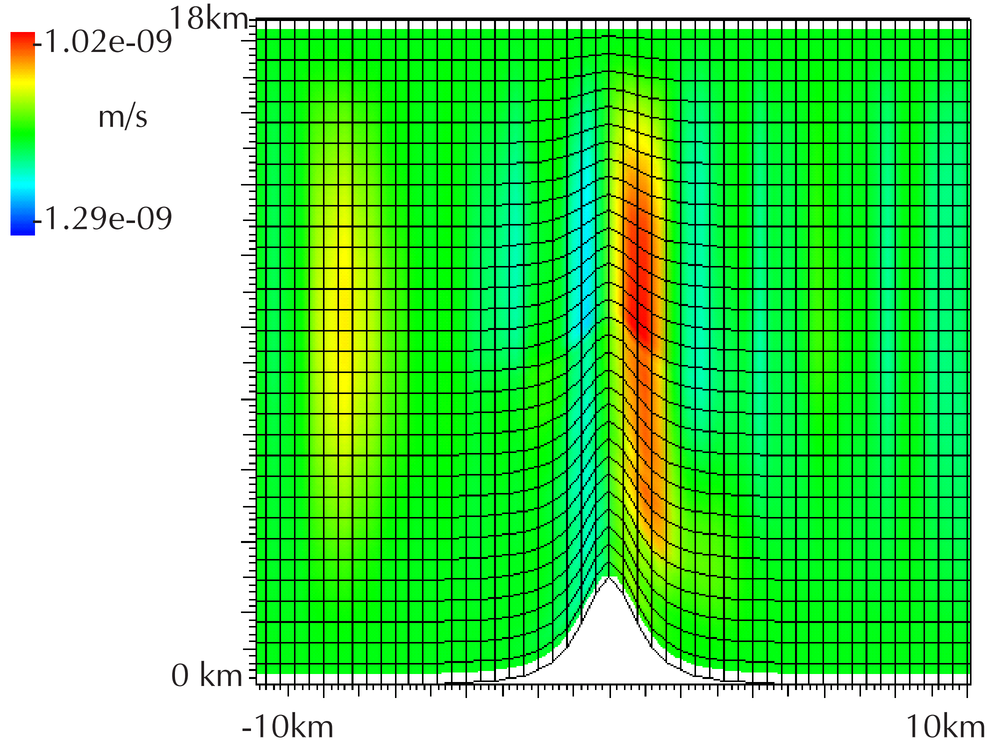


***No** accumulation of unbalanced truncation errors*

# Inversion layers at a mid-mountain level

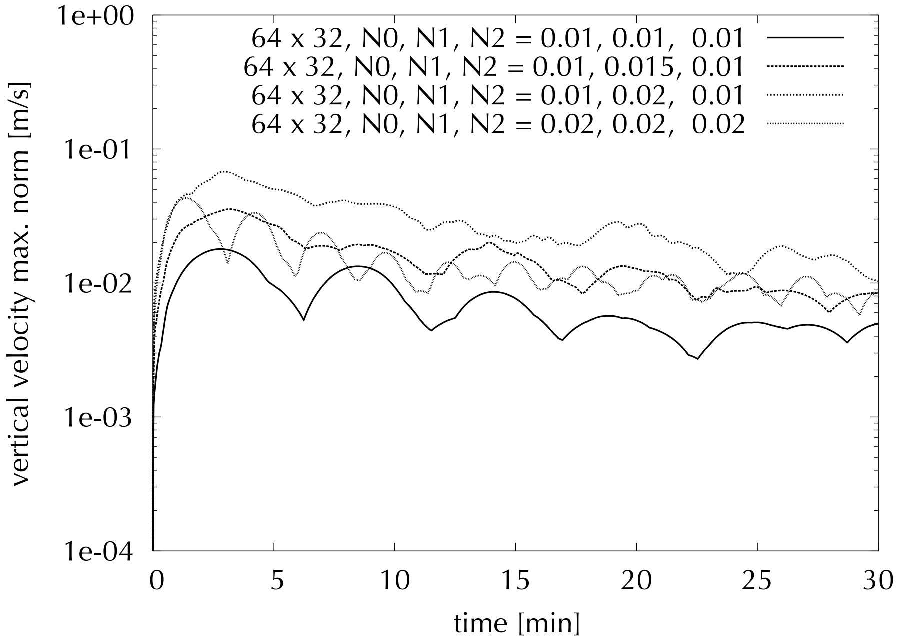


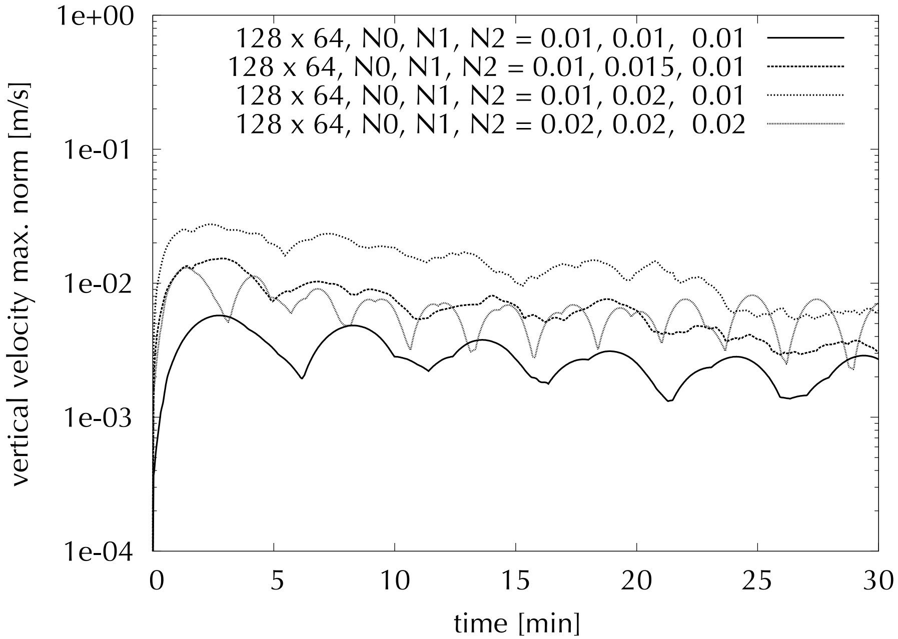


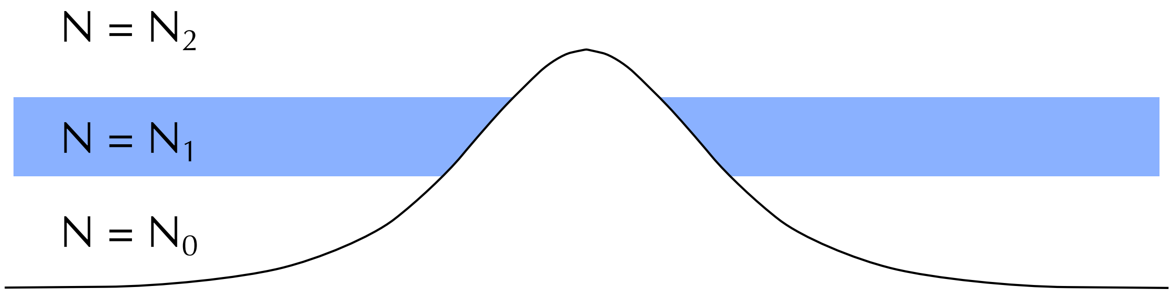


***No* accumulation of unbalanced truncation errors**

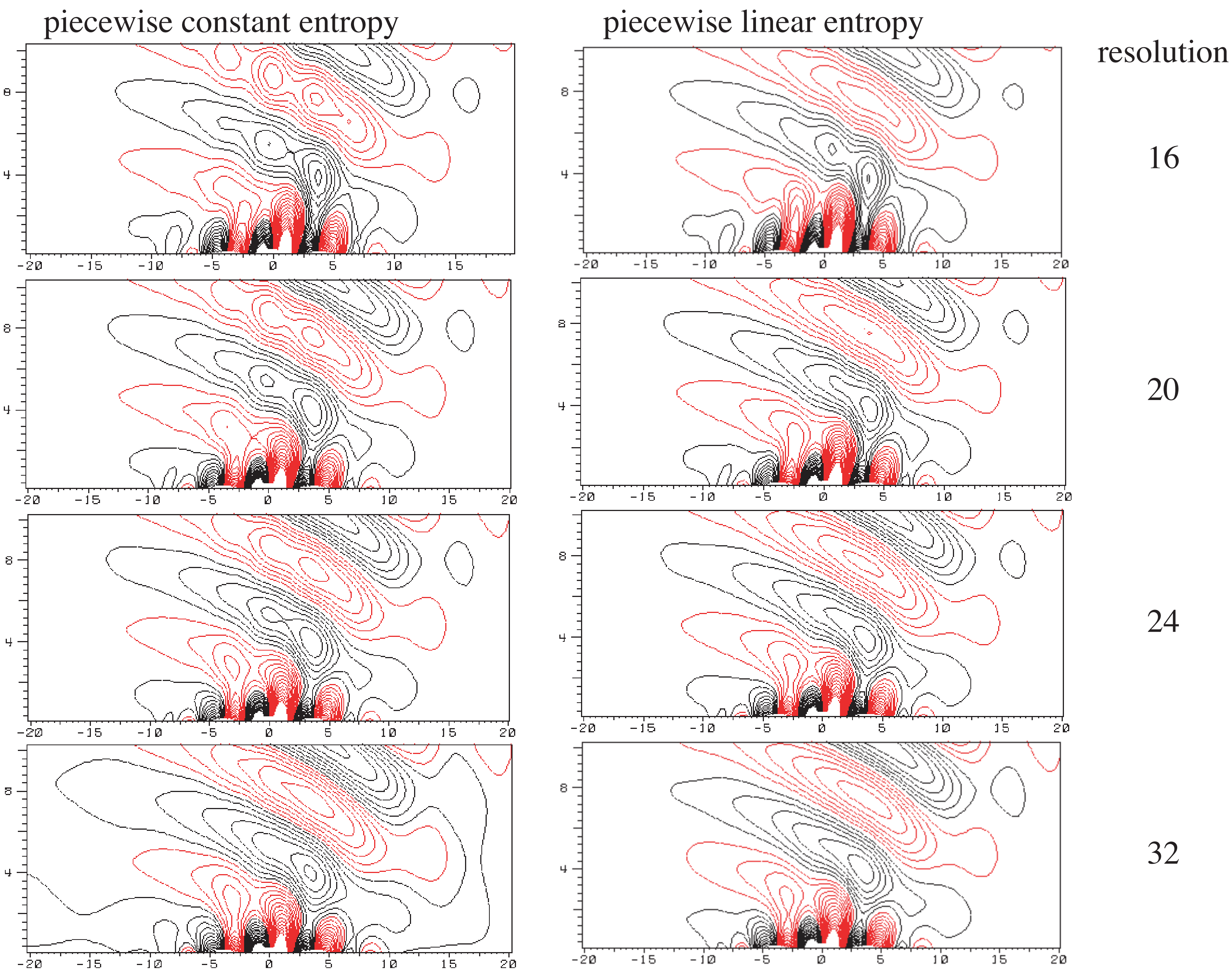


N. Botta, et al.: Well-Balanced Finite Volume Methods for Near-Hydrostatic Flows, JCP, (2004)

# *Convergence vs. marginal resolution (Schaer's Test)*

Motivation

Balancing gravity

**Momentum conservation vs. Coriolis**

A low-Mach / low-Froude conservative scheme

- low Mach number Godunov-Type scheme
- robust, exact projection
- low-Froude extension

The Coriolis **source**-term

$$2\,\boldsymbol{\Omega} \times \rho\boldsymbol{v}$$

is the result of a coordinate transformation.

Standard numerical discretizations do not maintain momentum conservation.

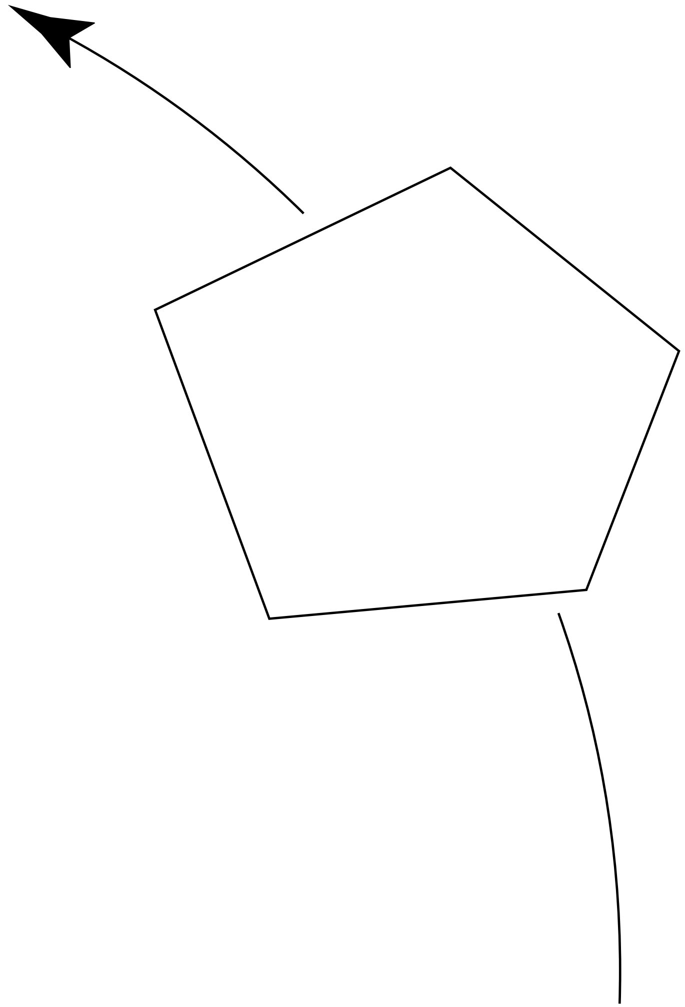

**Idea:** Apply coordinate transformation to **conservative moving grid discretization** in the inertial frame.

$$2\,\boldsymbol{\Omega} \times \rho\boldsymbol{v} \;\Rightarrow\; \text{rotationterm} + \text{fluxterm}$$

(work in progress with **E. Audusse**)

**Shallow water version (1st order)**

$$h_i^{n+1} \;=\; h_i^n - \frac{\Delta t}{|C_i|} \sum_j F_{ij}^h$$

$$\begin{aligned}
\boldsymbol{q}_i^{n+1} \;=\; & \underline{R(\Delta t)\boldsymbol{q}_i^n} - h_i^{n+1}\boldsymbol{\Omega} \times \boldsymbol{x}_i + h_i^n R(\Delta t)\boldsymbol{\Omega} \times \boldsymbol{x}_i \\
& - \frac{\Delta t}{|C_i|} \sum_j \boldsymbol{F}_{ij}^q \\
& \underline{- \frac{\Delta t}{|C_i|} \sum_j \left( F_{ij}^h \boldsymbol{\Omega} \times \boldsymbol{x}_{ij} \right)}
\end{aligned}$$

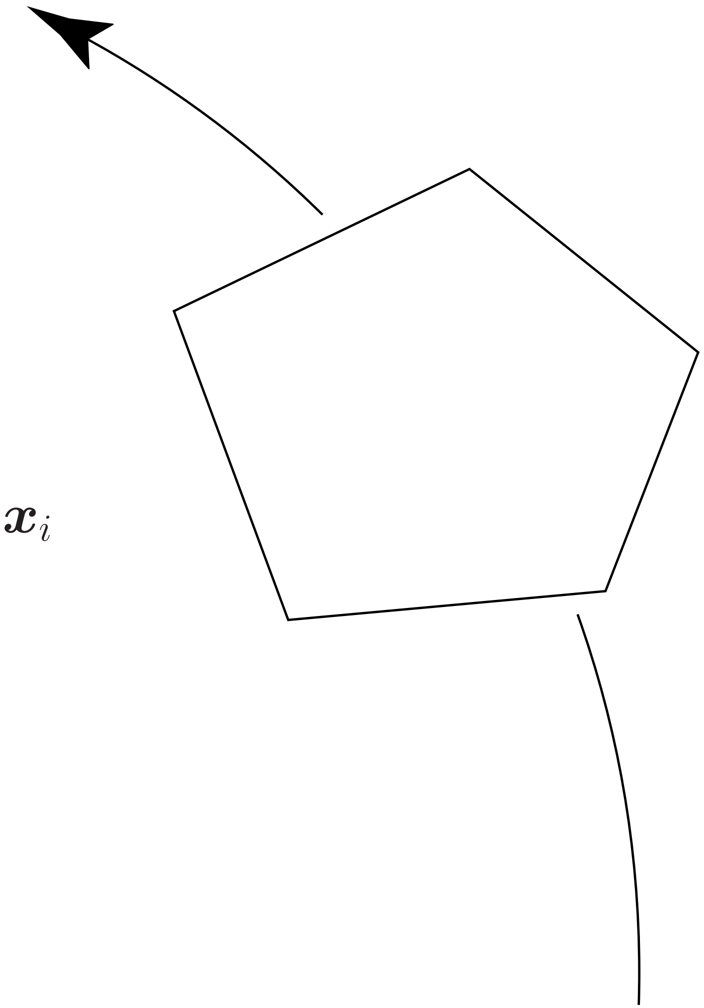

## *Momentum conservation vs. Coriolis*

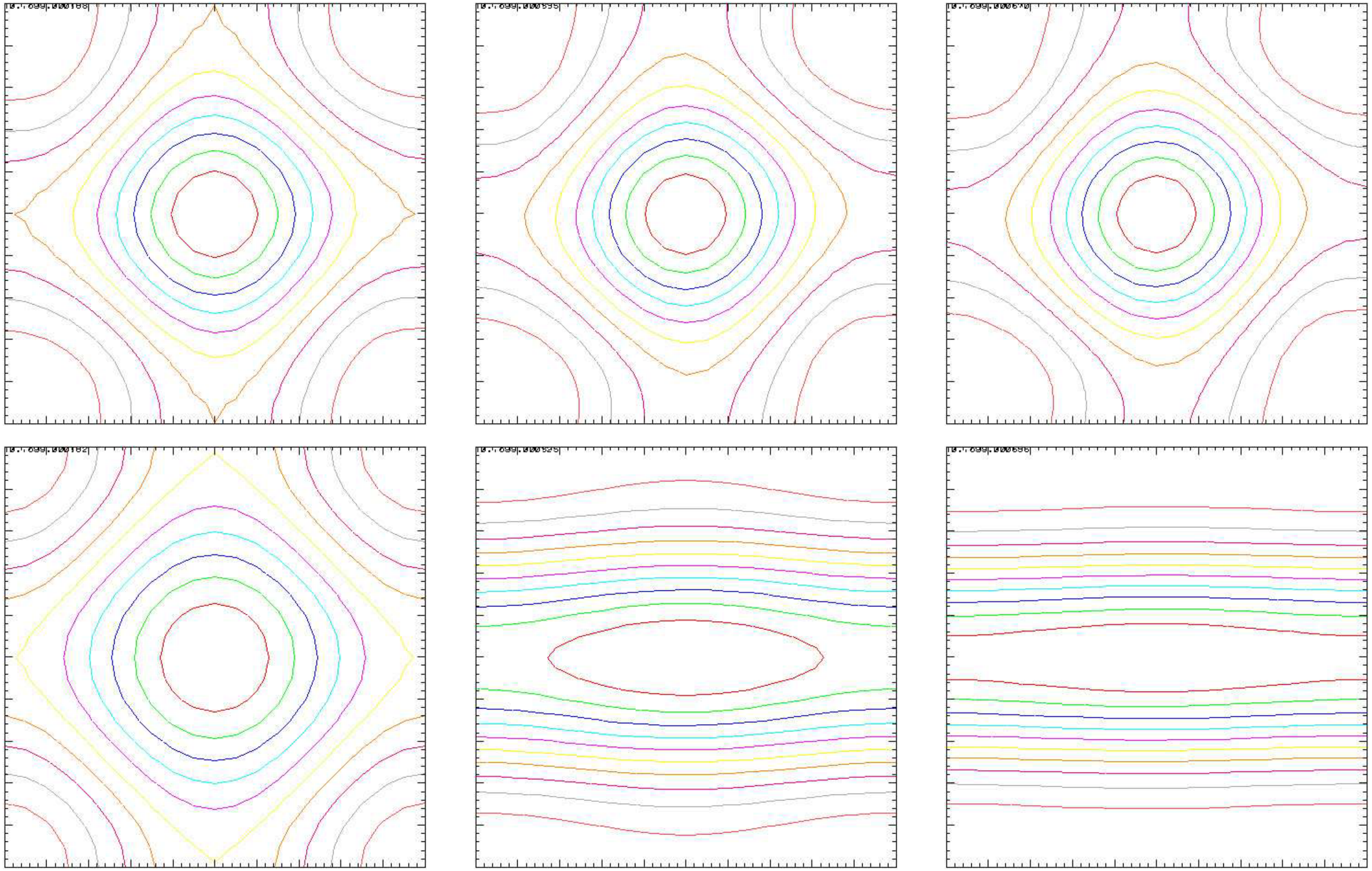

Water height for stationary vortex test:

Top: Cross-wind scheme, Bottom: Standard scheme

left to right: 20 cells horizontal / 20, 40, 80 cells in the vertical

## *Momentum conservation vs. Coriolis*

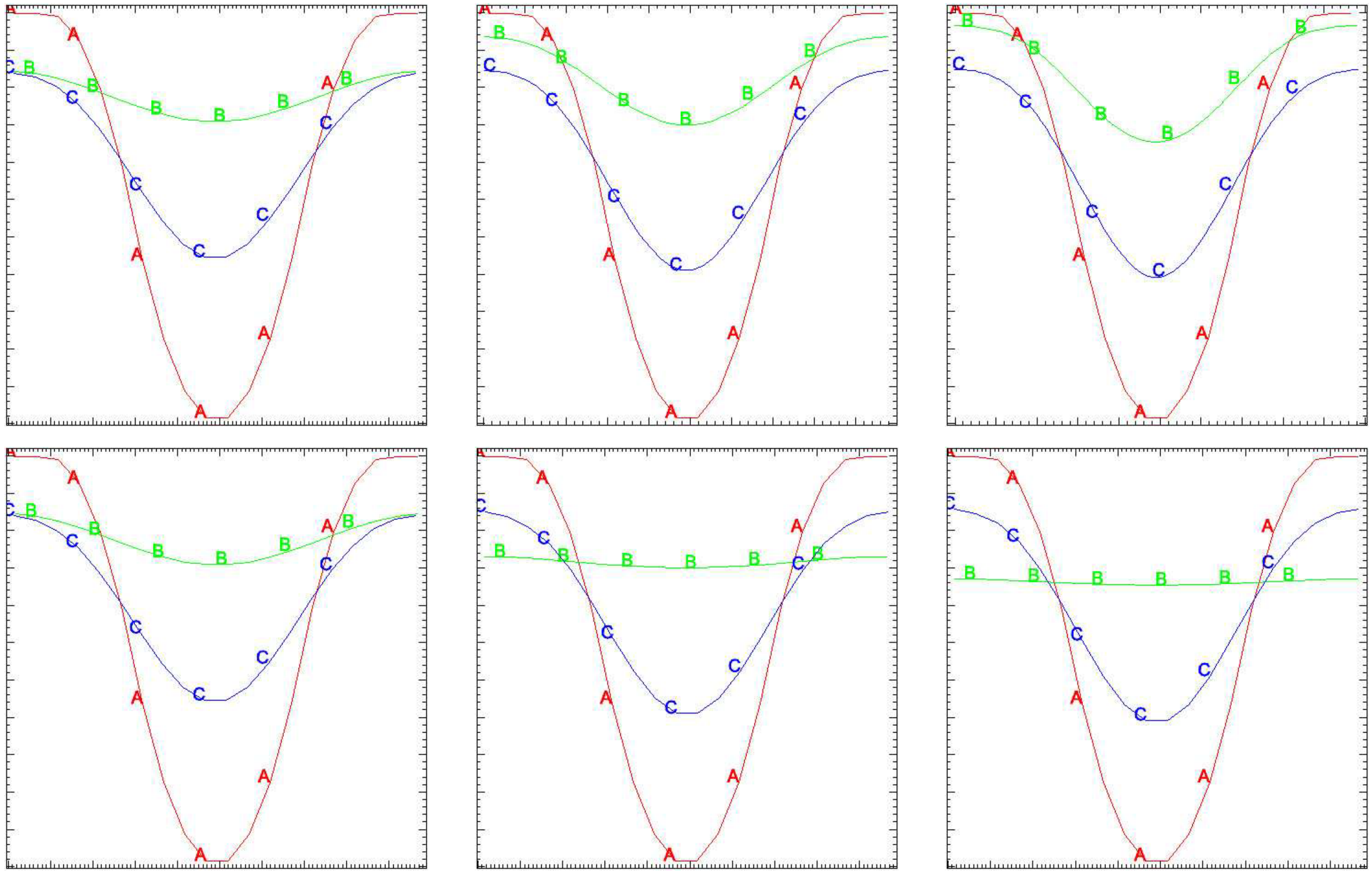


Water height for stationary vortex test:

Top: Vertical cross section, Bottom: Horizontal cross section

left to right: 20 cells horizontal / 20, 40, 80 cells in the vertical

initial data, cross-wind scheme, standard scheme

*Momentum conservation vs. Coriolis*

Motivation

Balancing gravity

Momentum conservation vs. Coriolis

**A low-Mach / low-Froude conservative scheme**

- **low Mach number Godunov-Type scheme**
- robust, exact projection
- low-Froude extension

## Three zero Mach number, anelastic regimes:

1. Inkompressible flow ( no gravity )

2. Ogura-Phillips-Anelastic flow ( $\theta = \mathbf{1} + \mathbf{M}^2\theta'$ )

3. Buoyancy-controlled flow ( $\theta = \boldsymbol{\Theta_0(z)} + \mathbf{M}^2\theta'$ )

## Regime 1: Incompressible flow

Leading order result:

$$p = P_\infty + \varepsilon^4 \boldsymbol{p'}$$

Consequences:

$$\rho e \quad = \quad \frac{p}{\gamma - 1} + \varepsilon^4 \frac{\rho \boldsymbol{v}^2}{2} \quad \longrightarrow \quad \frac{P_\infty}{\gamma - 1} \qquad (\varepsilon \longrightarrow 0)$$

$$(\rho e)_t + \nabla \cdot ([\rho e + p]\boldsymbol{v}) = 0 \qquad \longrightarrow \qquad \nabla \cdot \boldsymbol{v}^{(0)} = 0$$

$$\rho_t + \nabla \cdot (\rho \boldsymbol{v}) = 0 \qquad \longrightarrow \qquad \rho_t^{(0)} + \boldsymbol{v}^{(0)} \cdot \nabla \rho^{(0)} = 0$$

$$(\rho \boldsymbol{v})_t + \nabla \cdot (\rho \boldsymbol{v} \circ \boldsymbol{v}) + \frac{1}{\varepsilon^4} \nabla p = 0 \qquad \longrightarrow \qquad (\rho \boldsymbol{v})_t^{(0)} + \nabla \cdot (\rho \boldsymbol{v} \circ \boldsymbol{v})^{(0)} + \nabla \boldsymbol{p'} = 0$$

## Task:

Construct a scheme for low Mach number flows, which ...

- conserves mass, momentum, and total energy,
- is at least second order accurate in space and time,
- requires the solution of at most linear, scalar equations (possibly a few of them per time step)
- reduces, for $\mathbf{M} = 0$, to the variable density, incompressible solver in Schneider et al., JCP, (1999)
- reduces, for $\mathbf{M} = 1$, to a second order Godunov-type scheme

## Explicit / implicit split for the Euler equations

(R.K., JCP (1995); M. Minion & R.K, (2005))

$$
\begin{aligned}
\rho_t \;+\; & \nabla\cdot(\rho\boldsymbol{v}) && = 0\\
(\rho\boldsymbol{v})_t \;+\; & \nabla\cdot(\rho\boldsymbol{v}\circ\boldsymbol{v}) + \nabla p + \underline{\left(\frac{1}{\mathbf{M}^2}-1\right)\nabla\boldsymbol{p_*}} && = 0\\
(\rho e)_t \;+\; & \nabla\cdot([\rho e + \boldsymbol{\pi}]\;\boldsymbol{v}) && = 0
\end{aligned}
$$

$$
\rho e = \frac{p}{\gamma-1} + \mathbf{M}^2\,\frac{\rho\boldsymbol{v}^2}{2}
$$

$$
\boldsymbol{\pi} = \underline{\left(1-\mathbf{M}^2\right)\boldsymbol{p_*}} + \mathbf{M}^2\,p
$$

## Energy balance (Divergence correction for energy fluxes)

$$\mathbf{M}^2 \left( \frac{1}{\Delta t} \left[ \frac{\delta \boldsymbol{p_*}'}{\gamma - 1} + \left( \frac{\rho \boldsymbol{v}^2}{2} \right) \Big|_n^{**} - \boldsymbol{v}^{**} \cdot \tilde{\nabla} \delta \boldsymbol{p_*}' \right] + (1 - \mathbf{M}^2) \tilde{\nabla} \cdot (\delta \boldsymbol{p_*}' \, \boldsymbol{v}^{**}) \right)$$

$$= \quad -\left( \tilde{\nabla} \cdot (\rho h^* \, \boldsymbol{v}^{**}) - \frac{\Delta t}{2} \tilde{\nabla} \cdot (h^* \, \tilde{\nabla} \delta p) \right)$$

$\mathbf{M} = 0 \quad \Rightarrow$ classical **linear** projection step

$\mathbf{M} \ll 1 \quad \Rightarrow$ **linear**, non-singular inclusion of weak compressibility

# Advected homentropic vortex at $\mathbf{M} = 0.2$

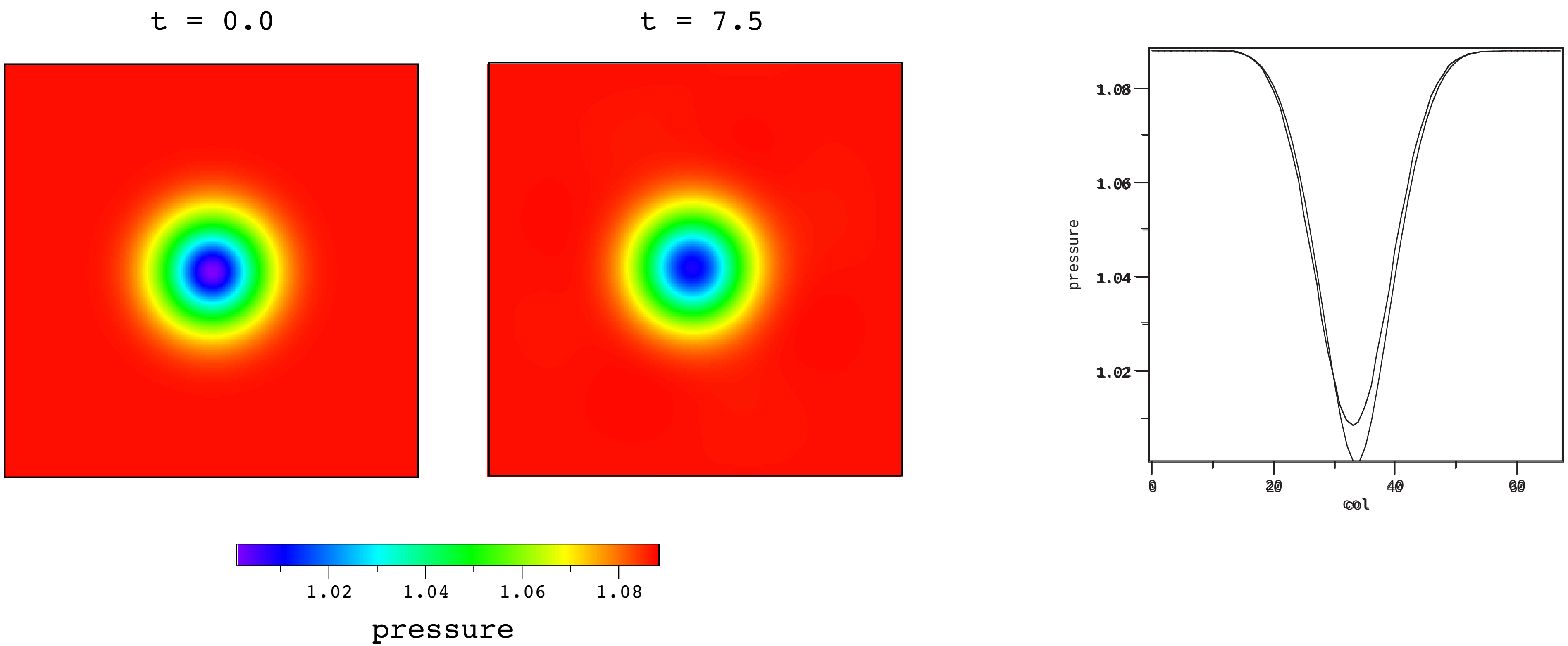


Convergence rates: $\boldsymbol{v} \to h^2$ , $p \to h^{1.5}$ , $\rho \to h^1$

Motivation

Balancing gravity

Momentum conservation vs. Coriolis

**A low-Mach / low-Froude conservative scheme**

- low Mach number Godunov-Type scheme
- **robust, exact projection**
- low-Froude extension

## Second projection: discrete approximations of $\boldsymbol{\nabla} \cdot \left(\dfrac{\mathbf{1}}{\boldsymbol{\rho}} \boldsymbol{\nabla} \boldsymbol{p}\right) = \boldsymbol{r}$

**Finite elements** (with test functions $\phi_{\boldsymbol{\nu}}$):

$$\forall \boldsymbol{\nu} : \qquad \int\limits_{\overline{\boldsymbol{C}}_{i,j}} \left[\frac{1}{\rho} \nabla p \cdot \nabla \phi_{\boldsymbol{\nu}} - r\, \phi_{\boldsymbol{\nu}}\right] \, dx = 0$$

where

$$p(x,y) = \sum_{\boldsymbol{\mu}} \hat{p}_{\boldsymbol{\mu}}\, \phi_{\boldsymbol{\mu}}$$

**Finite volumes** on dual cells

$$\oint\limits_{\boldsymbol{\partial \overline{C}}_{i,j}} \frac{1}{\rho} \nabla p \cdot \boldsymbol{n} \;\, d\sigma \;\; - \int\limits_{\overline{\boldsymbol{C}}_{i,j}} r \; dx = 0$$

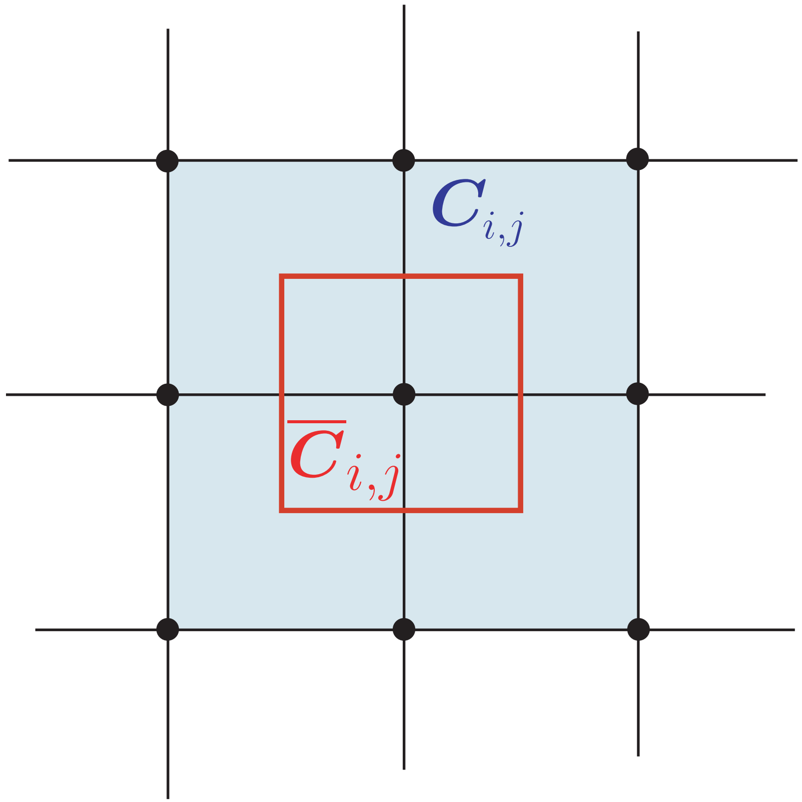


Bilinear pressure on FV-cells $\boldsymbol{C}_{i,j}$

***Bilinear pressure distributions: FE vs. FV stencil***

# Example: (robust, second order)* stencils for $\Delta p = \nabla \cdot \nabla\, p$

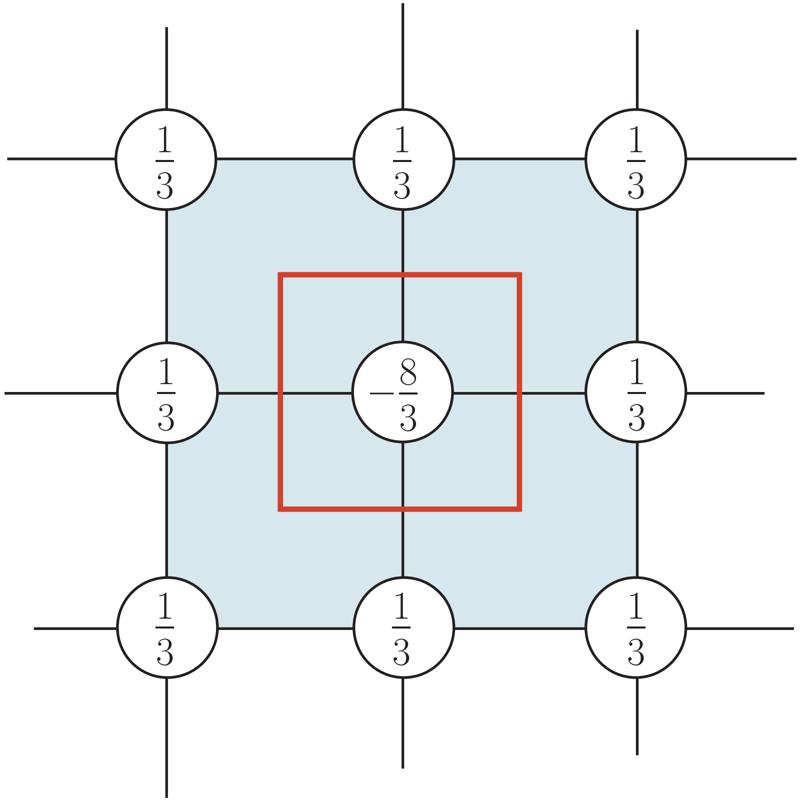


Conforming **finite elements**

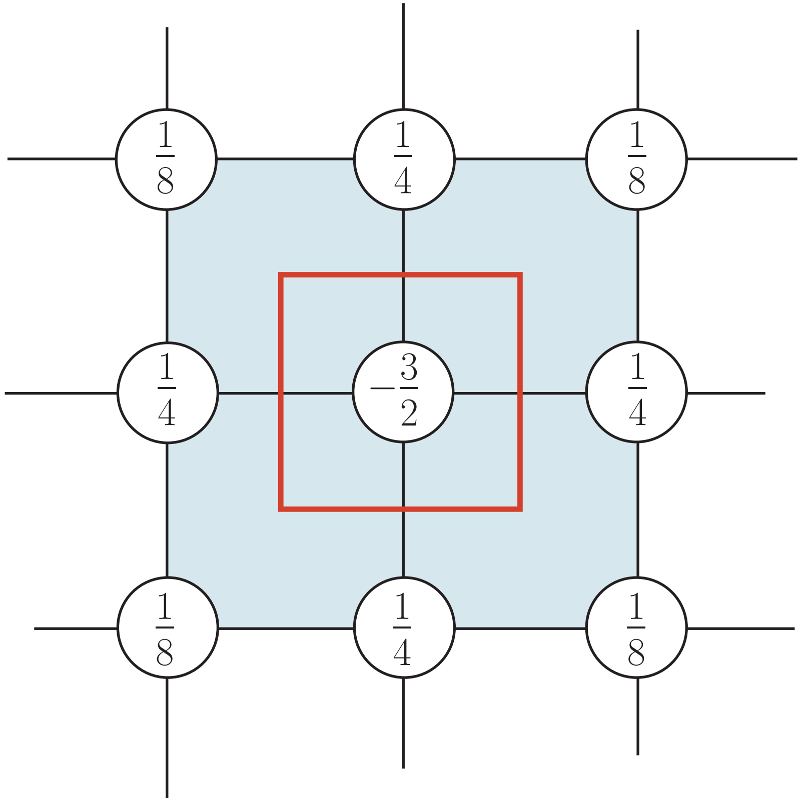


**Finite volumes** on dual cells:

* E. Süli: SIAM J. Num. Analysis, 28(5):1419-1430, 1991.

## Cell averaged updates

$$(\rho \boldsymbol{v})^{n+1}_{i,j} = (\rho \boldsymbol{v})^{*}_{i,j} - \Delta t \begin{pmatrix} \left(\partial_x p^{(2)}\right)_{i,j} \\ \left(\partial_y p^{(2)}\right)_{i,j} \end{pmatrix}$$

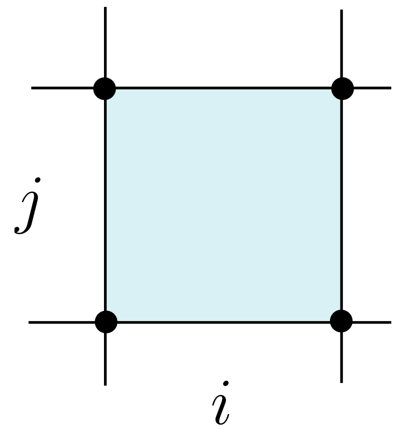


**conservative** gradient approximation, e.g.,

$$\left(\partial_x p^{(2)}\right)_{i,j} \approx \frac{1}{2\Delta x}\left(\left[p_{i+\frac{1}{2},j+\frac{1}{2}} + p_{i+\frac{1}{2},j-\frac{1}{2}}\right] - \left[p_{i-\frac{1}{2},j+\frac{1}{2}} + p_{i-\frac{1}{2},j-\frac{1}{2}}\right]\right)$$

**Local updates** within cells $C_{i,j}$:

$$(\rho \boldsymbol{v})^{n+1}(x,y) = (\rho \boldsymbol{v})^{*}(x,y) - \Delta t \, \nabla p^{(2)}(x,y)$$

where

$$\nabla p^{(2)}(x,y)\Big|_{i,j} = \begin{pmatrix} \left(\partial_x p^{(2)}\right)_{i,j} + (y - y_j)\left(\boldsymbol{\partial^2_{xy} p^{(2)}}\right)_{\boldsymbol{i,j}} \\ \left(\partial_y p^{(2)}\right)_{i,j} + (x - x_i)\left(\boldsymbol{\partial^2_{xy} p^{(2)}}\right)_{\boldsymbol{i,j}} \end{pmatrix}.$$

**Second projection modifies piecewise linear reconstruction:**

$$\left(\boldsymbol{\partial_x(\rho v)}\right)^{\boldsymbol{n+1}}_{\boldsymbol{i,j}} = \left(\partial_x(\rho v)\right)^{*}_{i,j} - \Delta t \left(\boldsymbol{\partial^2_{xy} p^{(2)}}\right)_{\boldsymbol{i,j}}$$

$$\left(\boldsymbol{\partial_y(\rho u)}\right)^{\boldsymbol{n+1}}_{\boldsymbol{i,j}} = \left(\partial_y(\rho u)\right)^{*}_{i,j} - \Delta t \left(\boldsymbol{\partial^2_{xy} p^{(2)}}\right)_{\boldsymbol{i,j}}$$

**Exact projection** achieved with:

$$(\nabla \cdot \boldsymbol{u})_{i,j}^{n+1} = \frac{1}{\left|\boldsymbol{\partial \overline{C}}_{i,j}\right|} \oint_{\boldsymbol{\partial \overline{C}}_{i,j}} \left(\frac{1}{\rho}\,\boldsymbol{m}\right)^{n+1} \cdot \boldsymbol{n} \;\; d\sigma$$

where

$$\boldsymbol{m}^{n+1}(x,y)\,\Big|_{i,j} = \begin{pmatrix} (\rho u)_{i,j}^{n+1} \; + \; (x - x_i) \quad \big(\partial_x(\rho u)\big)_{i,j}^{*} \quad + \; (y - y_j) \; \boldsymbol{\Big(\partial_y(\rho u)\Big)_{i,j}^{n+1}} \\ (\rho v)_{i,j}^{n+1} \; + \; (x - x_i) \; \boldsymbol{\Big(\partial_x(\rho v)\Big)_{i,j}^{n+1}} \; + \; (y - y_j) \quad \big(\partial_y(\rho v)\big)_{i,j}^{*} \end{pmatrix}$$

Motivation

Balancing gravity

Momentum conservation vs. Coriolis

## A low-Mach / low-Froude conservative scheme

- low Mach number Godunov-Type scheme
- robust, exact projection
- **low-Froude extension**

## Regime 3: Buoyancy-controlled anelastic flow $\theta = \boldsymbol{\Theta_0}(z) + \mathbf{M}^2\boldsymbol{\theta'}$

Leading order results:

$$p = \boldsymbol{P}_0(z) + \mathbf{M}^2\boldsymbol{p'} \qquad \rho = R_0(z) + \mathbf{M}^2\boldsymbol{\rho'} \qquad R_0(z) = \boldsymbol{\Theta_0}(z)\ \boldsymbol{P}_0(z)^{1/\gamma}$$

Consequences:

$$\rho e \quad = \quad \frac{p}{\gamma - 1} + \mathbf{M}^2\frac{\rho \boldsymbol{v}^2}{2} + \rho g z \quad \to \quad \frac{\boldsymbol{P}_0(z)}{\gamma - 1} + R_0(z) g z \qquad (\mathbf{M} \to 0)$$

$$(\rho e)_t + \nabla \cdot ([\rho e + p]\boldsymbol{v}) = 0 \qquad \to \qquad \nabla \cdot \left(\boldsymbol{v}^{(0)} R_0(z) \left[\frac{\gamma}{\gamma - 1}\frac{\boldsymbol{P}_0}{R_0}(z) + g z\right]\right) = 0$$

$$\rho_t + \nabla \cdot (\rho \boldsymbol{v}) = 0 \qquad \to \qquad \nabla \cdot \left(\boldsymbol{v}^{(0)} R_0(z)\right) = 0$$

**Un**fortunately

$$\left[\frac{\gamma}{\gamma - 1}\frac{\boldsymbol{P}_0}{R_0} + g z\right] \equiv \boldsymbol{\Phi(z)} \not\equiv \text{const.} \quad \Rightarrow \quad \nabla_{||} \cdot \boldsymbol{u}^{(0)} = 0, \quad \text{and} \quad w^{(0)} = 0$$

## Regime 3: Buoyancy-controlled anelastic flow $\theta = \mathbf{\Theta_0}(z) + \mathrm{\mathbf{M}}^2 \boldsymbol{\theta'}$

Leading order results:

$$p = \boldsymbol{P_0}(z) + \mathrm{\mathbf{M}}^2 \boldsymbol{p'} \qquad \rho = R_0(z) + \mathrm{\mathbf{M}}^2 \boldsymbol{\rho'} \qquad R_0(z) = \mathbf{\Theta_0}(z)\ \boldsymbol{P_0}(z)^{1/\gamma}$$

Consequences (cont'd):

$$(\rho \boldsymbol{v})_t + \nabla\cdot(\rho \boldsymbol{v} \circ \boldsymbol{v}) + \frac{1}{\mathrm{\mathbf{M}}^2}(\nabla p + \rho g) = 0 \quad \longrightarrow \quad (\rho \boldsymbol{v})_t^{(0)} + \nabla\cdot(\rho \boldsymbol{v} \circ \boldsymbol{v})^{(0)} + (\nabla \boldsymbol{p'} + \boldsymbol{\rho'}) = 0$$

$(\boldsymbol{P_0}, \mathbf{\Theta_0}, \boldsymbol{p'}, \boldsymbol{\rho'})$ must be maintained as primary variables in a numerical implementation

## Generalization to anelastic regimes:

**Energy balance** (**Divergence correction for energy fluxes**)

$$\mathbf{M}^2 \left( \frac{1}{\Delta t} \left[ \frac{\delta \boldsymbol{p_*}'}{\gamma - 1} + \left. \left( \frac{\rho \boldsymbol{v}^2}{2} \right) \right|_n^{**} - \Delta t \, \boldsymbol{v}^{**} \cdot \tilde{\nabla} \delta \boldsymbol{p_*}' \right] + (1 - \mathbf{M}^2) \tilde{\nabla} \cdot (\delta \boldsymbol{p_*}' \, \boldsymbol{v}^{**}) \right)$$

$$= \quad - \left( \tilde{\nabla} \cdot (\rho h^* \, \boldsymbol{v}^{**}) - \frac{\Delta t}{2} \tilde{\nabla} \cdot \left(h^* \, \left[ \tilde{\nabla} \delta \boldsymbol{p_*}' + \delta \boldsymbol{\rho_*}' \boldsymbol{k} \right] \right) \right)$$

**Mass balance** (**Divergence correction for mass fluxes**)

$$\frac{\mathbf{M}^2}{\Delta t} \delta \boldsymbol{\rho_*}' = - \left( \tilde{\nabla} \cdot (\rho^* \, \boldsymbol{v}^{**}) - \frac{\Delta t}{2} \tilde{\nabla} \cdot \left( \left[ \tilde{\nabla} \delta \boldsymbol{p_*}' + \delta \boldsymbol{\rho_*}' \boldsymbol{k} \right] \right) \right)$$

Potential Temperature:

$$\theta = \frac{p^{\frac{1}{\gamma}}}{\rho}$$

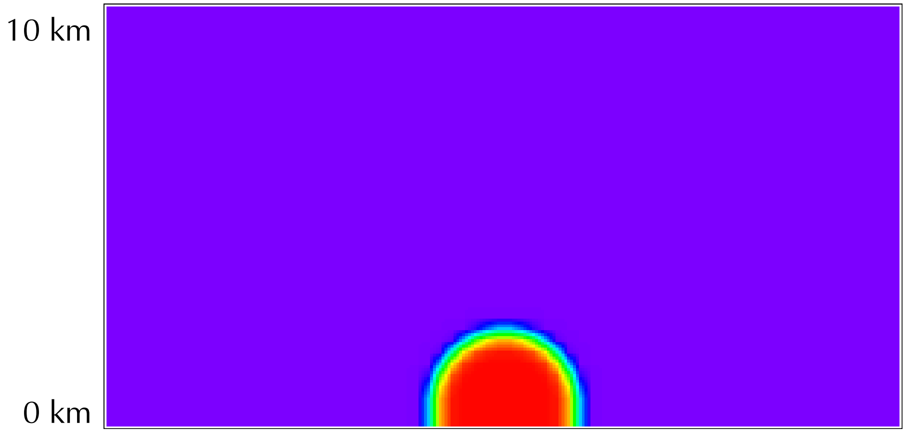


Rising thermal plume ($\delta\theta/\theta = 0.1$) in a 10 km neutral atmosphere

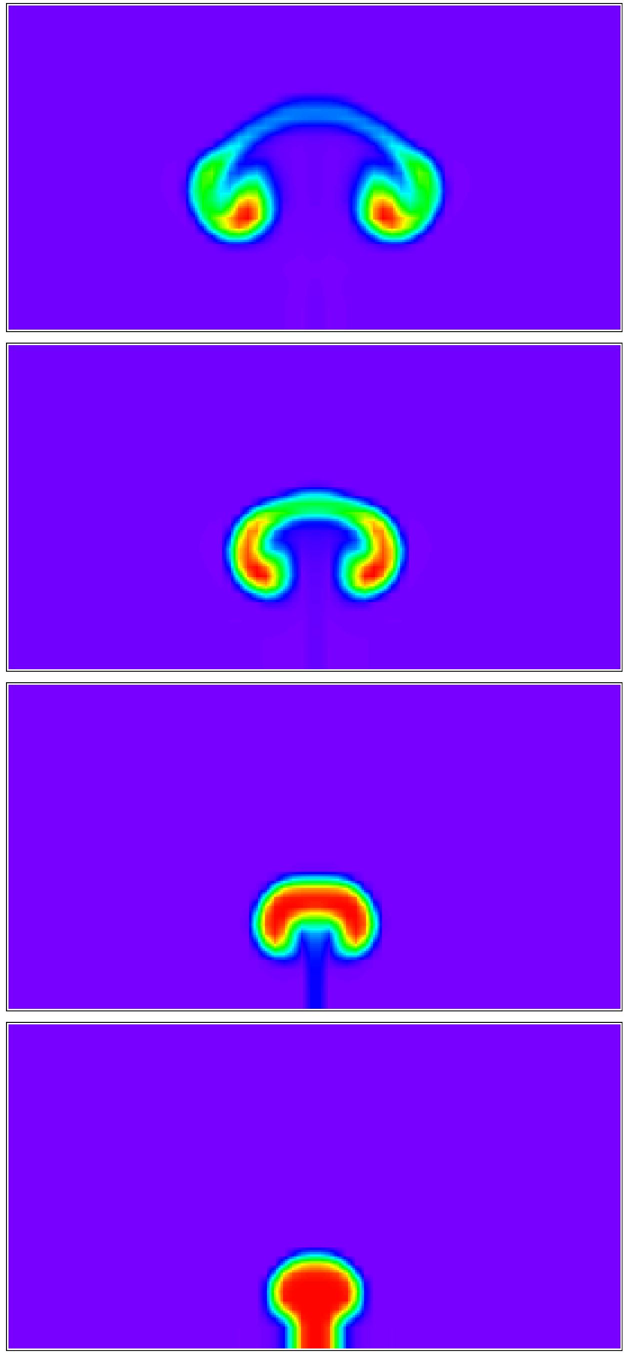

# Conclusions